

Dalton Transactions

Accepted Manuscript



This is an *Accepted Manuscript*, which has been through the Royal Society of Chemistry peer review process and has been accepted for publication.

Accepted Manuscripts are published online shortly after acceptance, before technical editing, formatting and proof reading. Using this free service, authors can make their results available to the community, in citable form, before we publish the edited article. We will replace this *Accepted Manuscript* with the edited and formatted *Advance Article* as soon as it is available.

You can find more information about *Accepted Manuscripts* in the [Information for Authors](#).

Please note that technical editing may introduce minor changes to the text and/or graphics, which may alter content. The journal's standard [Terms & Conditions](#) and the [Ethical guidelines](#) still apply. In no event shall the Royal Society of Chemistry be held responsible for any errors or omissions in this *Accepted Manuscript* or any consequences arising from the use of any information it contains.



Journal Name

ARTICLE

Planar Tetracoordinate Carbon in Tungstenacyclobutadiene of Alkyne Metathesis and Expanded Structures

Premaja R. Remya^{†,‡} and Cherumuttathu H. Suresh^{*†,‡}Received 00th January 20xx,
Accepted 00th January 20xx

DOI: 10.1039/x0xx00000x

www.rsc.org/

Planar tetracoordinate (p_tC) character of C_β in the tungstenacyclobutadiene (WCBD) of alkyne metathesis is analyzed with the support of structural, electronic, molecular orbital and electron density data obtained from density functional theory calculations. The p_tC character of C_β is due to 1,3-WC bonding which is established on the basis of single bond-like WC_β distance in X-ray structures and calculated structures, catastrophe ring critical point for the WCBD ring in quantum theory of atoms-in-molecule analysis (QTAIM) and large difference in ^{13}C -NMR data of C_α and C_β atoms. The metalloaromatic character of WCBD is revealed from nuclear independent chemical shift (NICS) values and diatropic ring current observed in the anisotropy of the induced current density plot (AICD). These WCBD structural motifs provide a new strategy to build 1-, 2- and 3-dimensional organometallic polymeric structures containing multiple p_tC centers. Several such structures are reported, and the 3-dimensional extensions of them provide access to novel p_tC -incorporated metal-organic framework.

Introduction

Ever since Hoffmann *et al.*¹ brought the concept of planar tetracoordinate carbon (p_tC) to world's attention, stabilization of a p_tC has been viewed as a fascinating challenge given to chemist. Hoffmann and co-workers proposed that stabilization of p_tC can be achieved either through a mechanical approach by constraining the geometry in such a way that the central carbon and its neighbours are in one plane or through an electronic approach by incorporating suitable substituents (ions, metal centers) where at least one of the coordinations should be an atom other than carbon.¹⁻³ Schleyer and co-workers proposed that stabilization of p_tC is also possible by incorporating the carbon to small ring systems.⁴⁻⁶ Another widely used approach for the stabilization of p_tC centers is through the introduction of transition metals. A divanadium complex of formula $V_2[(OMe)_2C_6H_3]_2$ was the first crystallographically characterized molecule to show a p_tC center.⁷ Later many bimetallic complexes containing p_tC centers have been reported with different metal centers like Ti, Pd, W, Re and Ce.⁸⁻¹³ Along with bimetallic systems, some monometallic complexes are known to possess p_tC centers where the planar tetracoordination results from the additional interaction of the carbon with the metal center.¹⁴ It was observed that in some zirconocene complexes the fourth bond of the carbon is the result of the CH agostic interaction with the metal center.^{15,16} Similar unusual bonding interactions were reported in the case of metallacyclobutadienes, metallacyclopentadienes, and other small metallacycles.¹⁷⁻²⁰

Many reviews dealing with the progress in the field of planar tetra- and hypercoordinate carbon systems are available in the literature.^{12, 21-25}

Recently, the metallacyclobutadiene (MCBD) intermediate of alkyne metathesis has been proposed as a p_tC complex wherein the p_tC center is the β -carbon of the MCBD.^{26,27} MCBD intermediates of alkyne metathesis especially with tungsten catalysts are stable, and many crystal structures²⁸⁻³⁰ are available in Cambridge structural database (CSD) and theoretical studies have also established them as minimum energy structures.^{31,32} Structurally, the p_tC nature of the MCBD is assigned on the basis of short single-bond like MC_β distance (2.20 – 2.40 Å). Based on energy decomposition, bond order and electron density analyses, the significant bonding interaction between metal and the β -carbon has been unambiguously proven in the case of a Schrock tungsten complex $Cl_3W(C-MeC-MeC-tBu)$ (CSD ID BONXOR) (Fig. 1a). This bond named as 1,3-MC bond provided the fourth coordination for the carbon along with three other bonds (two CC and one CH bonds) in the plane of the metallacycle (Fig. 1).²⁶

Three decades ago, Schrock *et al.* reported the unexpected formation of 'deprotio' metallacycles during the course of metathesis reaction of terminal alkynes with molybdenum and tungsten catalysts.^{33,34} For instance, the reaction of $WCp(C-tBu)Cl_2$ with $C-tBuCH$ in triethyl amine yielded the metallacycle $WCpCl[C-tBuCC-tBu]$ (CSD ID CEGGAW, Fig. 1a) instead of the expected MCBD $WCpCl_2[C-tBuC-HC-tBu]$ due to dehydrohalogenation. Short WC_β distance of 2.049 Å in $WCpCl[C-tBuCC-tBu]$, indicated bond formation. Recently Jemmis *et al.* have studied structurally similar group 4 'deprotio' metallacycles known as metallacycloallenes using molecular orbital and natural bond orbital analyses and confirmed that four-membered metallacycloallenes are

^{†,‡} Chemical Sciences and Technology Division, CSIR-National Institute for Interdisciplinary Science and Technology, Trivandrum 695 019, India †Academy of Scientific & Innovative Research, CSIR-National Institute for Interdisciplinary Science and Technology, Trivandrum 695 019, India. E-mail: sureshch@niist.res.in Electronic Supplementary Information (ESI) available: [QTAIM data, QTAIM figures, orbital pictures, optimized geometries etc.]. See DOI: 10.1039/x0xx00000x

stabilized through metal- C_{β} bonding interaction.³⁵ Although the C_{β} of metallocycloallene or a 'deprotio' metallacycle is not a ptC center (only 3 atoms, *viz.* two C_{α} and the metal center are bonded to C_{β}), WCpCl[C-tBuCC-tBu] has been considered in this study to assess the strength of the 1,3-MC type interaction in the MCBD.

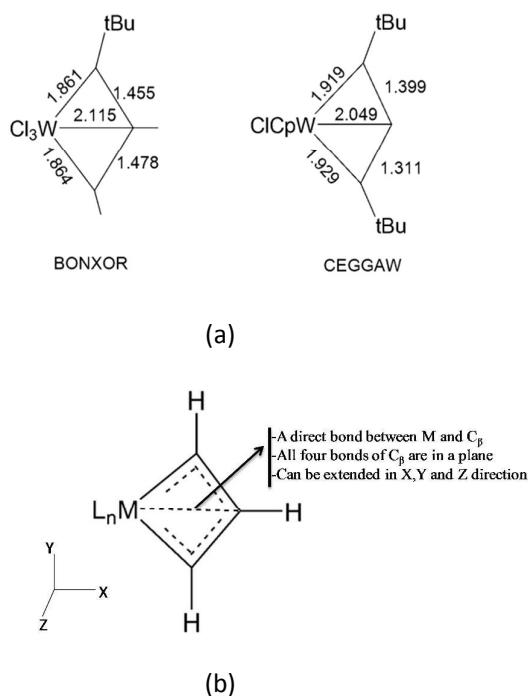


Fig. 1 (a) Molecular drawings of the crystal structures of tungstenacyclobutadiene, BONXOR and 'deprotio' tungstenacyclobutadiene, CEGGAW (b) Schematic representation of a bond between metal and C_{β} in an MCBD complex.

Recently, Suresh and Frenking showed the existence of 1,3-MC bond in the MCBD systems of group 4, 5 and 6 transition metals.^{26, 27} This bonding is due to considerable d_{π} - p_{π} interaction^{36, 37} between the metal and C_{β} and this finding paved the way for a new type of ptC chemistry in organometallics. Compared to the previous theoretical and experimental discoveries on ptC centers, the finding that a ptC center is available in MCBD is more fascinating because of the role it plays in alkyne metathesis reaction as well as the status of the complex as a well-defined, stable, structurally characterized organometallic complex. MCBD system can also be viewed as a system wherein the metal center is incorporated into a small carbon framework. Such metallic incorporation in carbon frameworks can drastically change the properties of the resulting molecules and on the basis of its new materials exhibiting interesting optical, electronic and magnetic properties can be designed and developed. Thus, the stable form of ptC in MCBD offers new design strategies for the development of ptC based materials. Using the extension of the building block in Fig. 1b, Suresh and Frenking have computationally designed "edge complexes" of group 4

transition metals by utilizing the 1,3-MC bonding at the edges of aromatic hydrocarbons.³⁸ Herein, we propose that the structural motif given in Fig. 1b for a ptC center can be extended to design more complex architectures in 1-, 2- and 3-dimensions. The larger structures can be envisaged by extending the structure in the X-, Y- and Z-direction via the β -carbon, α -carbon and the metal center, respectively (Fig. 1b). Many computational attempts have been made in the past to design the possible extension of molecules possessing multiple ptC centers in complex networks.^{24, 39-42} Prediction of edge decorated graphene systems possessing ptC centers is also proposed by many groups by incorporating metal centers and some non-metals.^{43, 44}

In this work, we want to emphasize that the ptC center, as well as the 1,3-MC bond observed in an MCBD system of alkyne metathesis is fundamental to organometallic chemistry and these findings immediately open up new room for expanding the chemistry of ptC through 1,3-MC bond in CC frameworks. We perform this study as a computational endeavour to the design of ptC incorporated metal-organic frameworks.

Computational details

For the optimization of crystal structures, and 1- and 2-dimensional structures, the BP86/BS1⁴⁵ level of density functional theory (DFT) is used wherein BS1 stands for triple-zeta quality basis set def2-tzvp for all the atoms and the use of effective core potential for W to treat the core electrons. For the optimization of large 3-dimensional cage structures, BP86/BS2⁴⁶ level is used wherein BS2 stands for the all electron basis set SDD with effective core potential for W and 6-31g* basis set for other elements. BP86 is a GGA functional containing Becke 1988 exchange functional and the Perdew 86 correlation functional.^{47, 48} All the calculations have been carried out with Gaussian09 program.⁴⁹ All the structures discussed in this work have been confirmed as energy minima by locating only positive frequency for all the normal modes of vibration unless otherwise specified. Wiberg bond order analysis⁵⁰ is done to quantify bond strength using Natural Bond Orbital analysis (NBO) as implemented in Gaussian09. Electron density topology analysis^{51, 52} is done with AIMALL program⁵³. For ¹³C-NMR analysis, GIAO method^{54, 55} in Gaussian09 is used. The same method is used to calculate Nucleus Independent Chemical Shift values at the center of the ring, NICS(0), at one Å above the ring center, NICS(1) and also the zz-tensor component of NICS(1), NICS(1)_{zz}.⁵⁶ Aromaticity of MCBD ring is visualized in terms of Anisotropy of Induced Current Density (AICD) developed by Herge's group.^{57, 58}

Results and discussion

At first we consider X-ray crystal structures of seven tungstenacyclobutadiene (WCBD) systems (Fig. 2) for the structural and bonding analysis to confirm the existence of 1,3-MC bond. Among them the first three systems, identified in

the CSD as WEMYIY, WEMYOE, and WEMYUK, are reported in a very recent work by Veige *et al.*⁵⁹ They have synthesized the first neutral trianionic ONO pincer-type tungsten alkylidyne complexes and showed that these complexes can react rapidly with alkynes to yield WCBDs. Though the possibility of 1,3-MC bond in these structures are obvious from the single bond-like WC_β distance (~ 2.15 Å), this kind of a bonding was not discussed by Veige *et al.* In Fig. 2, we also depict the schematics of the molecular geometries of WCBD systems reported by Schrock and co-workers and identified in CSD as COMREB¹⁷, CONISH¹⁸ and CUYJEL¹⁹. Yet another WCBD system is KISGID reported by Tamm *et al.*³⁰ In Table 1, the bond length (WC_α , WC_β and $C_\alpha C_\beta$) and bond angle ($C_\alpha C_\beta C_\alpha$) parameters of the metallacycle region are depicted for the X-ray structures and the corresponding theoretically derived structures.

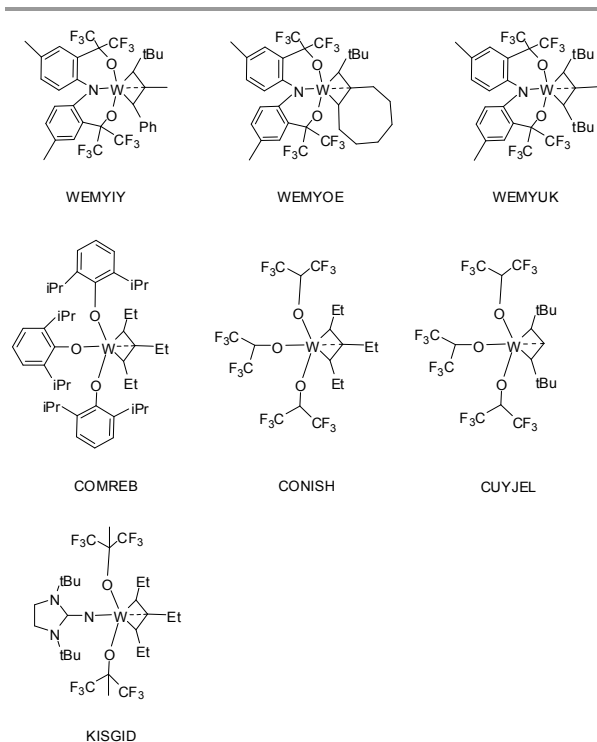


Fig. 2 Molecular drawing of the crystal structures of tungstenacyclobutadienes. CSD ID is used to name the molecules.

None of the structures show any kind of symmetry as they possess dissimilar WC_α and $C_\alpha C_\beta$ bond distances. It is gratifying that the computed values of the distance particularly the WC_β distance and bond angles (Table 1) show good agreement with experimental values. In addition to the σ -type bonding interaction between W and C_α , the π -type interaction between metal d-orbitals and the carbon p-orbital gives substantial double bond character to the WC_α bond. As a result, WC_α bonds show significantly shorter distance than the typical WC_α single bond (2.10 Å). The strongest evidence that support the existence of 1,3-MC bond in these complexes is the single bond-like WC_β distance. Both theory and experiment agree that the WC_β distance in the range 2.093 – 2.234 Å is well

within the sum of the van der Waals radii of tungsten and carbon (~ 3.8 Å) and is comparable with the WC_β distance in the 'deprotio' metallacycle CEGGAW (2.05 Å). The good agreement between the gas phase optimized WC_β data and the corresponding crystal data clearly suggest that the single bond-like WC_β distance cannot be neglected as a consequence of structural restriction imposed in the four-membered ring or due to crystal packing.

Table 1 Structural parameters of WCBD in the crystal and in the optimized geometries given in parenthesis (bond distances are given in Å and angles in degree).

MCBD	WC_α	WC_β	$C_\alpha C_\beta$	$C_\alpha C_\beta$	WC_β	$\angle C_\alpha C_\beta C_\alpha$
WEMYIY	1.905 (1.935)	1.911 (1.943)	1.450 (1.452)	1.473 (1.468)	2.159 (2.192)	119.9 (120.5)
WEMYOE	1.897 (1.930)	1.911 (1.938)	1.443 (1.450)	1.473 (1.467)	2.156 (2.185)	119.9 (120.5)
WEMYUK	1.882 (1.927)	1.908 (1.936)	1.453 (1.459)	1.456 (1.464)	2.143 (2.185)	120.0 (120.3)
COMREB	1.883 (1.903)	1.949 (1.986)	1.433 (1.417)	1.466 (1.490)	2.159 (2.193)	120.8 (121.0)
CONISH	1.864 (1.926)	1.903 (1.930)	1.428 (1.436)	1.437 (1.481)	2.093 (2.164)	122.5 (121.3)
CUYJEL	1.890 (1.939)	1.921 (1.942)	1.417 (1.428)	1.499 (1.466)	2.103 (2.134)	123.1 (124.3)
KISGID	1.879 (1.901)	1.992 (2.024)	1.387 (1.397)	1.533 (1.519)	2.209 (2.234)	119.3 (120.0)

QTAIM analysis

In the QTAIM parlance, affirmation of the bonding interaction between two atoms is verified by locating a (3, -1) critical point (known as bond critical point (BCP)) and the associated atomic interaction line (known as the bond path (BP)) between the interacting atoms. The issue on the use of BP as a universal indicator of bonding is highly debated in the literature and many people have commented that the detection of a BP or BCP is not necessary to verify the bonding interaction between two atoms.⁶⁰⁻⁶⁷

In the QTAIM analysis, a BCP or BP is not observed between tungsten and C_β for any of the tungstenacyclobutadienes listed in Fig. 2. All of them showed a characteristic ring critical point (RCP) for the metallacycle. The QTAIM molecular graphs given for the optimized geometries of WEMYUK and CUYJEL in Fig. 3 along with contours of Laplacian of electron density are useful to understand typical electron density features of the metallacyclobutadiene. Very similar molecular graphs have been obtained for all other systems (ESI). As seen in these molecular graphs, at the RCP, the four ring paths coming from the surrounding four BCPs do not meet sharply as expected for a normal ring structure. Instead, the RCP region is characterized by flat curvature for the ring paths. Previously, Suresh and Frenking showed that such a feature of RCP can be associated with the catastrophe nature of the critical point.²⁷ At the catastrophe point, the possibility of the merging of RCP and BCP exists if one of the eigenvalues of the RCP is very close to zero. Previously, it was shown that such a catastrophe nature can be resolved by adjusting the metal- C_β

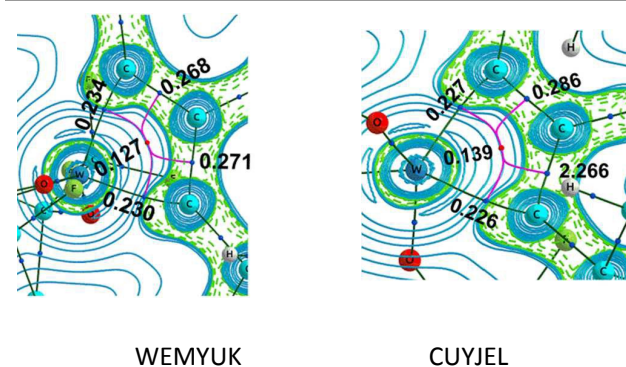


Fig. 3 Molecular graphs of WEMYUK and CUYJEL, showing a flat curvature for the meeting point of ring paths along the contours of Laplacian of electron density. Only metallacycle region is shown for clarity and ρ values are in au.

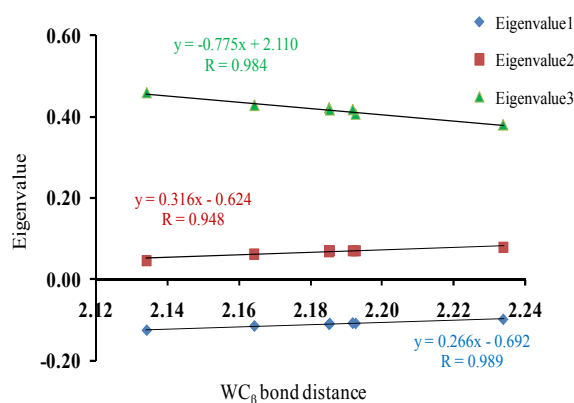


Fig. 4 Correlation between WC_{β} bond distances (\AA) and eigenvalues (au) at the catastrophe RCP of various WCBD structures.

distance to a slightly smaller value than the optimized value as this will lead to the formation of a BCP and the associated BP.^{27, 68} Thus presence of a catastrophe critical point can be considered as the indication of bonding interaction between the metal and C_{β} . In Table 2, the three eigenvalues of the catastrophe RCP are given. Since the RCP is designated as a (3, +1) critical point, one of the eigenvalues has to be negative and the other two have to be positive. As we can see, one of the positive eigenvalues is very close to zero (eigenvalue 2) which can be considered as an indicator of the catastrophe nature of the RCP. Hence, the system that shows the lowest positive eigenvalue must have the highest catastrophe character. The smallest positive eigenvalue may become negative with sufficiently strong interaction between W and C_{β} which will give rise to a (3, -1) BCP critical point.

In Fig. 4, the variation of the eigenvalues with change in the WC_{β} distance for various optimized crystal structures is presented. The linear plots given in this figure clearly suggest that with increase in the WC_{β} interaction, the most positive eigenvalue (eigenvalue 3) becomes more positive, the least positive eigenvalue (eigenvalue 2) becomes smaller while the magnitude of the negative eigenvalue (eigenvalue 1) remain almost a constant. On the basis of this figure, we can assume

that among all the structures, CUYJEL has the highest amount of 1,3-MC bonding character. By extrapolating the eigenvalue plots in Fig. 4, a value $\sim 1.98 \text{ \AA}$ for WC_{β} distance can be suggested at which the system may show a BCP along with a clear BP between W and C_{β} . To check this, we reduced the WC_{β} distance of CUYJEL manually and at a distance of 1.99 \AA (a saddle point in the potential energy surface) a clear BCP was found along with a BP connecting W and C_{β} (ESI). Thus it is apparent that the absence of a BCP does not indicate the absence of a bonding interaction. Molecular orbital pictures of WEMYUK given in ESI prove that the 1,3-MC interaction is mainly arising from significant $d_{\pi}-p_{\pi}$ interaction between W and C_{β} .

Table 2 QTAIM parameters calculated for the WCBD systems and the 'deprotio' metallacycle CEGGAW.

MCBD	AIM parameters (au)			Eigenvalue at RCP (au)		
	WC_{α} BCP	$C_{\alpha}C_{\beta}$ BCP	WC_{β} RCP	1	2	3
WEMYIY	0.230	0.271	0.126	-0.108	0.071	0.417
WEMYOE	0.232	0.272	0.129	-0.111	0.070	0.421
WEMYUK	0.232	0.270	0.127	-0.109	0.071	0.416
COMREB	0.226	0.274	0.125	-0.109	0.071	0.406
CONISH	0.232	0.272	0.132	-0.115	0.064	0.428
CUYJEL	0.226	0.276	0.139	-0.125	0.047	0.459
KISGID	0.219	0.274	0.116	-0.099	0.079	0.379
CEGGAW	0.218	0.297	0.176	-0.197	-0.020	0.485

Among the QTAIM parameters given in Table 2, the most important in the analysis of 1,3-MC bond are those associated with the catastrophe RCP. The ρ at the RCP is in the range 0.116 - 0.139 au. This indicates significant build up of electron density between W and C_{β} . In the case of the 'deprotio' metallacycle CEGGAW, a BCP is observed between W and C_{β} with ρ value of 0.176 au. This can be considered as a well defined 1,3-MC bond in a metallacycle. Although the C_{β} of CEGGAW is tri-coordinate, the ρ value of its WC_{β} bond is useful to compare the strength of the 1,3-MC bond of the WCBD. The WCBD systems are 20 - 34 % smaller than the BCP ρ value of CEGGAW and indicates that the 1,3-MC interaction in the former is proportionally weaker than the latter. In all the metallacycles reported in Table 2, WC_{α} and $C_{\alpha}C_{\beta}$ bonds possess some amount of double bond character and their BCP ρ values show significantly higher values than a typical WC single bond (0.165 au) and a typical CC single bond (0.240 au).

Among all the WCBD structures given in Fig. 2, a C_{β} -H bond is present only in CUYJEL and this system showed the highest ρ value at the catastrophe RCP. Schrock *et al.* have reported the removal of alcohol from this system, leading to the formation of 'deprotio' metallacycle.⁶⁹ The optimised structure of the 'deprotio' metallacycle of CUYJEL is an energy minimum and in the QTAIM analysis it molecule showed a clear BCP with ρ value 0.175 au for the WC_{β} bond of length 2.074 \AA (ESI).

Bond order analysis

Table 3 Wiberg bond order calculated for MCBd in the optimized geometries of MCBd.

MCBD	Wiberg bond order				
	WC _α	WC _β	C _α C _β	C _α C _β	WC _β
WEMYIY	1.385	1.356	1.256	1.175	0.348
WEMYOE	1.386	1.416	1.261	1.181	0.355
WEMYUK	1.419	1.405	1.220	1.222	0.351
COMREB	1.511	1.227	1.358	1.082	0.356
CONISH	1.370	1.450	1.280	1.134	0.395
CUYJEL	1.363	1.430	1.308	1.170	0.422
KISGID	1.119	1.603	1.473	1.035	0.286

The bond order parameters depicted in Table 3 strongly augment the conclusions drawn from the structural data and QTAIM analysis that tungsten is bonded to C_β for the 1,3-WC bonding. All the WCBD structures show WC_β bond order in the range 0.286 – 0.422 which suggests significant bonding interaction between W and C_β. The CUYJEL system composed of alkoxide ligand has the highest WC_β bond order 0.422. KISGID with imidazolin imidato ligand has the smallest WC_β bond order 0.286 whereas the pincer ligand incorporated structures of Veiga *et al.* show WC_β bond order ~0.35.

¹³C-NMR analysis**Table 4** ¹³C-NMR values calculated for MCBd in the optimized geometries of MCBd.

MCBD	¹³ C-NMR			
	δC _α	δC _β	δC _α - δC _β	δC _α - δC _β
WEMYIY	205.3	218.4	144.8	67.1
WEMYOE	200.4	225.6	152.5	60.5
WEMYUK	207.0	234.7	147.4	73.5
COMREB	204.4	199.3	144.0	57.8
CONISH	199.6	213.6	154.2	52.4
CUYJEL	208.6	222.8	137.0	78.7
KISGID	213.7	214.0	134.4	79.4

Schrock *et al.* proposed the use of ¹³C-NMR chemical shift as a measure of WC_β interaction in the case of metallacyclobutane intermediates of alkene metathesis.⁷⁰ Similar ¹³C-NMR analysis has been used by Romero and Piers to prove the formation of ruthenacyclobutane intermediate in the Grubbs alkene metathesis mechanism, as the difference in the chemical shifts observed for the C_α and C_β were very large.⁷¹ Very recently we have shown that such behaviour can be attributed to the unusual penta-hypercoordinate bonding character of C_β in the MCB. ⁶⁸ In this work, the structure of interest is MCBd. Because of the unusual πC bonding character of C_β, a large difference in the chemical shift values of C_α (δC_α) and C_β (δC_β) is expected for MCBd. This is indeed true and in all the cases, the NMR signal of C_β is 52 - 79 ppm smaller than that of C_α (Table 4) which is in agreement with the

experimental data (ESI). The 1,3-MC bonding shields the C_β more than C_α leading to more upfield shift for C_β than the C_α. We propose that the large difference in the ¹³C-NMR values of C_α and C_β can be considered as a signature of 1,3-MC bonding in the metallacycle.

Table 5 Various NICS indices calculated for MCBd in the optimized geometries of MCBd.

MCBD	NICS(0)	NICS(1)	NICS(1) _{zz}
WEMYIY	-25.8	-15.4	-36.8
WEMYOE	-25.8	-15.4	-45.3
WEMYUK	-25.8	-15.1	-34.7
COMREB	-28.9	-17.4	-33.9
CONISH	-28.3	-16.1	-44.7
CUYJEL	-30.1	-17.2	-37.8
KISGID	-26.0	-15.9	-39.4

The elucidation of crystal structures of several MCBd systems of alkyne metathesis clearly suggest that they possess superior stability compared to the 4-membered anti-aromatic cyclobutadiene.⁷² It is well known that anti-aromatic to aromatic transformation of organic moieties can be obtained by the incorporation of a transition metal center via chelating effect.^{73, 74} Aromatic character of such systems is known as metalloaromaticity.⁷⁵ Erdman and Lawson⁷⁶ studied metalloaromaticity in tungstenacyclobutadiene using computational techniques and reported that the nucleus independent chemical shift at the ring center, NICS(0) is -28 ppm for the Schrock's MCBd crystal, BONXOR. The high negative NICS(0) value suggested aromatic stabilization of the MCBd. Apart from NICS(0), NICS at 1 Å above the ring center, NICS(1) and its zz-tensor component NICS(1)_{zz} have also been used for the study of aromatic nature of a molecule. In Table 5, the NICS(0), NICS(1) and NICS(1)_{zz} of all the complexes are reported which may be compared with those of benzene (NICS(0) = -7.8, NICS(1) = -10.8 and NICS(1)_{zz} = -28.1), a reference for a typical aromatic molecule. NICS(0) in the range -26 to -30 ppm is close to the value reported by Erdman and Lawson for BONXOR and indicate strong metalloaromatic character of these systems. The high negative values of NICS(1) and NICS(1)_{zz} compared to benzene also indicate the substantial stabilization of the former due to metalloaromaticity.

Very recently Herges group developed a methodology to calculate anisotropy of induced current density (AICD) maps and used it to quantify and visualize electron delocalization and aromaticity in molecules.^{57, 58} The AICD isosurface plot with current density vectors plotted on it gives either diatropic (clockwise) or paratropic (anti-clockwise) circulation of the current density depending on the aromatic or anti-aromatic nature of the molecule. Fig. 5 depicts such plots to visualize aromatic features for two representative cases, viz. WEMYUK and CUYJEL. It is clear from these plots that the MCBd systems possess aromatic delocalization of the π-electrons.

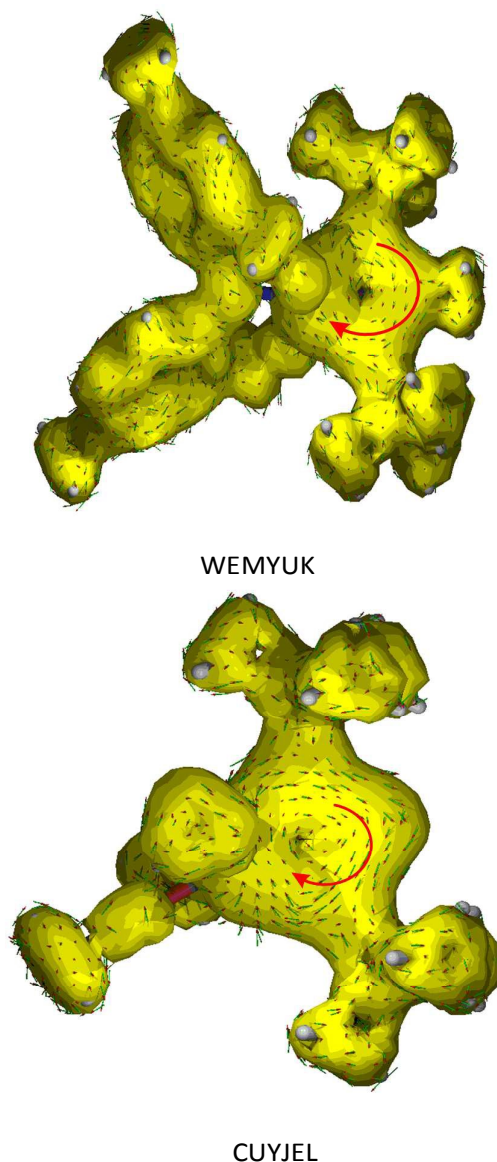


Fig. 5 AICD isosurface of WEMYUK and CUYJEL (isosurface value is 0.025). The current density vectors plotted on the isosurface shows clockwise circulation (diatropic), indicating aromatic character of the molecule. To clearly indicate the direction of the vectors, a curved red arrow is inscribed in the picture.

Systems with more than one MCB

Structural, electronic and bonding analyses of the known WCBBD structures confirm that the interaction between W and C_{β} can be considered as a direct bond. This new WC_{β} bond generally called as 1,3-MC bond defines the planar tetracoordinate state of C_{β} . Since several WCBBD structures exist in stable form, the 1,3-MC bond which contributes to their stability can be utilized to incorporate ptC centers in organometallic complexes. Although, the theoretical exploration of ptC chemistry is advanced to some extent, the

realistic application of a system containing ptC centers is yet to be achieved. Our results suggest that the consideration of WCBBD systems as ptC systems bring in more options to the design of realistic organometallic systems. To explore this revealing thought, we propose the use of tungstenacyclobutadiene as a basic building block to construct complex organometallic structures containing multiple ptC centers. The structural motif given in Fig. 1b is useful to illustrate the strategies used to develop such expanded systems in one-, two- and three-dimensions and the proposed models are given in Fig. 6.

Assuming the X-direction as the direction of the WC_{β} bond, extension of the structure in that direction can be envisaged by connecting two WCBBD structures similar to the known chloro-ligated Schrock system BONXOR through the β carbon as shown for model **1**. In **1**, the C_{β} of the two metallacycles are bonded with a distance of 1.479 Å and the two metallacycles show a symmetric orthogonal arrangement. The WC_{β} distance 2.169 Å in **1** is similar to any of the 1,3- WC_{β} bond distance given in Table 1. Further, the WC_{α} bond distance 1.923 Å indicates its double bond character while CC bond distance 1.446 Å indicates significant activation of that bond compared to a typical CC double bond (1.33 Å) or a conjugated aromatic CC bond (1.40 Å). We also consider the formation of two 1,3-WC bonded metallacycles around one tungsten atom. This model **2** is a minimum and both metallacycles in this complex show the characteristic 1,3-WC bond distance of 2.152 Å.

Expansion of the metallacycle in the Y-direction (more towards the direction of C_{α}) leads to the construction of two types of complexes, viz. **3** and **4**. The **3** is constructed by connecting C_{α} of two metallacycles whereas, in **4**, the C_{β} of one metallacycle serves as the C_{α} of the other metallacycle meaning that a CC bond is shared by both the metallacycles. Rosenthal *et al.* and many others reported complexes of type **4** and Schematics of such structures are reported in the ESI.^{20, 77, 78} Single bond like WC_{β} distance of 2.167 and 2.174 Å located respectively for **3** and **4** underlines the presence of 1,3-MC interaction in these complexes.

Polymeric 1-dimensional extension of the dimetallacycles **2** - **4** is possible while such an extension of **1** has to be compromised due to chloro ligation. Transition metal acetylide complexes are well discussed in the literature and by using acetylide units to connect metal centers, the linear expansion of **1**-type architecture can also be achieved and the model for such a structure is **5**.⁷⁹⁻⁸¹ Model **6** is made by connecting two units of **2** via the C_{β} . The one-dimensional extension of **3** is used to construct **7** while such an extension of **4** would lead to the formation of **8**. All these structures are energy minima, and all of them show single bond-like WC_{β} distances indicating the presence of 1,3-MC bonding. In **7** and **8**, the carbon chain resembles that of a polyene chain suggesting that these systems could be even considered as metal-incorporated polyene. All these extended structures preserve the 1,3-MC bonding features of metallacycles.

Journal Name

ARTICLE

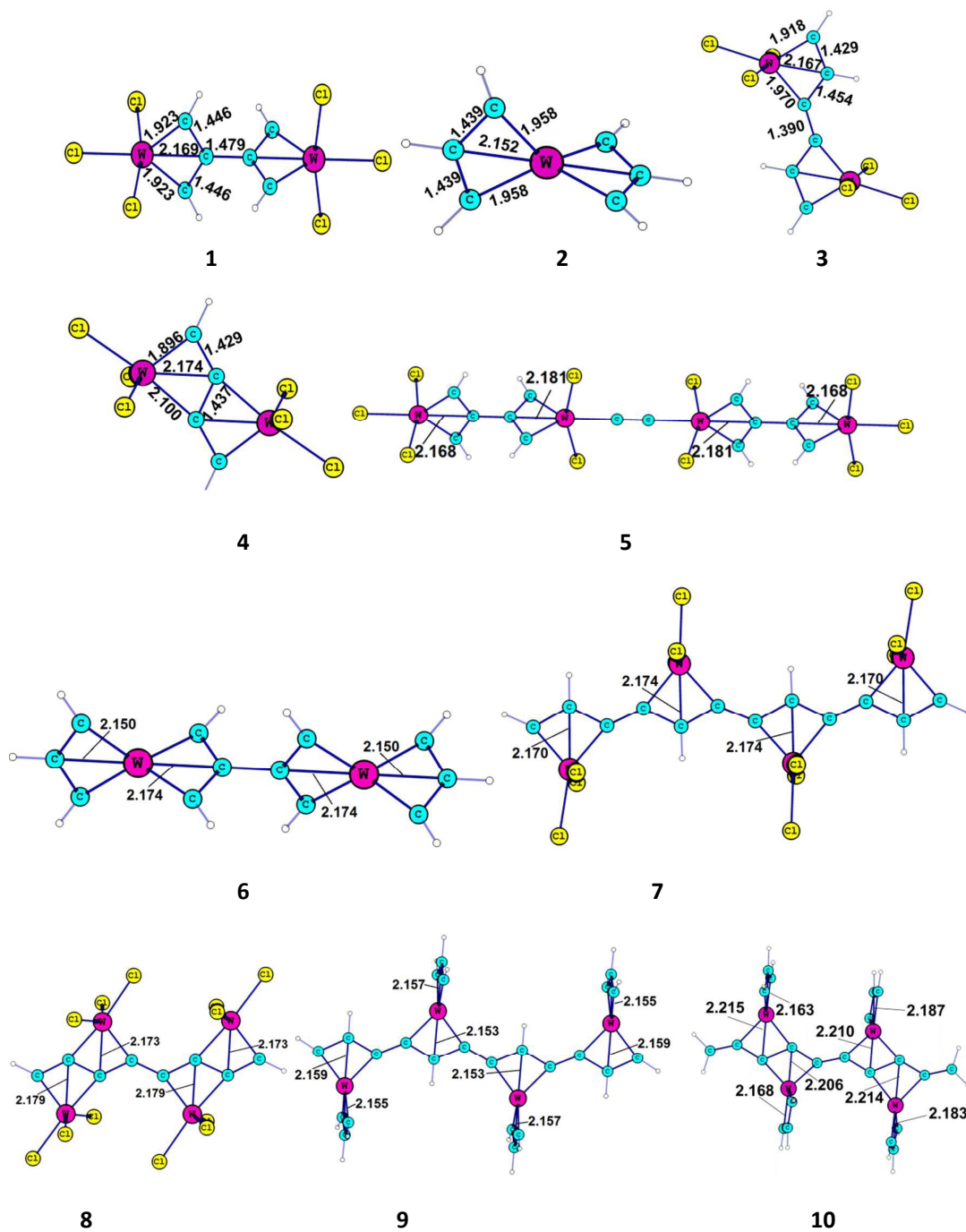
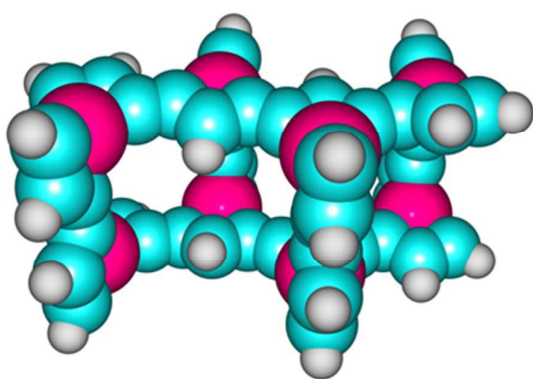
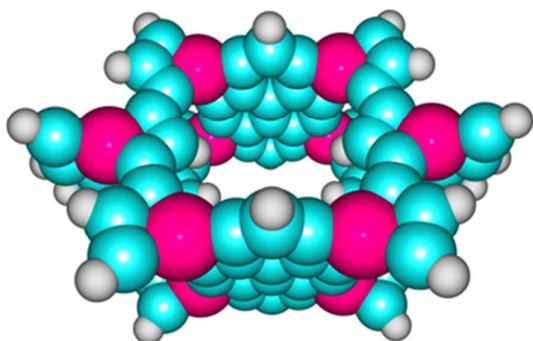


Fig. 6 Models containing more than one metallacycle unit.

Table 6 Wiberg bond order, QTAIM parameters, ^{13}C -NMR parameters calculated for the dimetallacycle models.

MCBD	Wiberg bond order					QTAIM parameters (au)					^{13}C -NMR			
	WC_α	WC_β	$\text{C}_\alpha\text{C}_\beta$	$\text{C}_\alpha\text{C}_\beta$	WC_β	WC_α BCP	WC_α BCP	CC BCP	CC BCP	WC_β RCP	δC_α	δC_α	δC_β	δC_β
1	1.466	1.465	1.208	1.209	0.371	0.236	0.236	0.278	0.278	0.131	199.8	199.8	152.2	152.2
2	1.274	1.274	1.301	1.302	0.384	0.218	0.218	0.278	0.278	0.135	193.6	193.6	133.9	133.9
3	1.452	1.234	1.281	1.167	0.399	0.239	0.215	0.287	0.274	0.132	194.0	197.4	145.2	145.2
4	1.499	0.765	1.157	1.192	0.477	0.249	0.165	0.28	0.277	0.135	163.7 ^a	163.7 ^a	151.8 ^b	151.7 ^b

^aterminal carbon, ^bmiddle carbon**11****12****Fig. 7** 3-dimensional WCBD complexes containing multiple ρ_{C} centers.

By combining the expansion patterns shown for the X- and Y-directions, two-dimensional expansions can be created. For instance, **9** is made by connecting **2** with **5**. Similarly, **10** can be made by combining **2** and **6** which can be further extended via the α -carbon or β -carbon. All the MCBD units in **9** and **10** possess single bond-like WC_β distances.

Wiberg bond order analysis on the dimetallacycles (Table 6) shows strong WC_β interaction in both WCBD region (0.371 –

0.477). Model **4** where one CC bond is shared between the two metallacycle showed the highest WC_β bond order of 0.477. The strongest (1.499) and the weakest WC_α (0.765) bonds are found in **4**. In all the cases, the CC bond order lies between 1.167 and 1.302. QTAIM analysis on these dimetallacycles (Table 6) showed a catastrophe ring critical point, where the ring paths meet with a flat curvature (ESI). The ρ value at the catastrophe point is nearly 0.133 au, which is close to a typical WC single bond value. Eigenvalue analyses of these models are discussed in the ESI, which confirms the catastrophe nature of the RCP.

Table 7 NICS parameters calculated for the dimetallacycles

MCBD	NICS(0)	NICS(1)	NICS(1) _{zz}
1	-27.7	-16.5	-25.0
2	-19.2	-7.2	-16.7
3	-28.9	-17.4	-45.3
4	-30.8	-17.1	-42.4

Negative values for all the three NICS indices (NICS(0), NICS(1) and NICS(1)_{zz}) have been observed for the dimetallacycles **1 - 4** (Table 7) indicating their metalloaromatic character. ^{13}C -NMR analysis on these molecules showed that α and β carbons are markedly different and suggest the presence of 1,3-MC bonding between metal and C_β . The QTAIM and NMR features of all the 1-dimensional (**5 - 8**) and 2-dimensional (**9 - 10**) extended structures are very similar to the dimetallacycles and suggest that C_β of WCBD region is 1,3-WC bonded and it exists in planar tetracoordinate state.

Further extension of 1- and 2-dimensional structures to 3-dimensional networks is possible through proper α - and β -carbon connectivity (Fig. 7). For example, **11** can be built from two units of **9**. Further, complex **12** can be made by combining two units of **9** along with two units of pyrene. As we can see, these type expansions of the WCBD structures can lead to the formation of metal-organic cavities in the system. In the case of **12**, a well-defined cavity of size (1.06, 0.81, 0.72 nm) in the

(X, Y, Z) directions is clearly seen. The 3-dimensional structures **11** and **12** also possess single-bond like WC_{β} distance ($\sim 2.2 \text{ \AA}$) and all the characteristic QTAIM and NMR features typically seen for a 1,3-WC bonded carbon atom.

Conclusions

Several tungstenacyclobutadienes available in the CSD have been studied for 1,3-WC bonding interaction. Single bond-like WC_{β} distance in these complexes is established with a significantly high bond order and appearance of a catastrophe ring critical point in the QTAIM analysis. Large negative NICS values obtained for these molecules point to their metalloaromatic character which is underlined with the diatropic ring current observed in the AICD plot. All these structures showed large difference in the ^{13}C -NMR signals of C_{α} and C_{β} which is considered as a characteristic feature of 1,3-WC bonding. Among the crystal structures, the alkoxide ligated complex CUYJEL reported by Schrock *et al.* showed the strongest WC_{β} interaction. In a constrained geometry, this model showed a clear bond critical point between W and C_{β} . This extra bonding interaction is further confirmed by molecular orbital analysis which clearly showed the $d_{\pi}-p_{\pi}$ interaction between tungsten and carbon. The 1,3-WC bonding in these metallacycles forces the C_{β} to exist in a planar tetracoordinate state, $p_{\pi}C$. Identification of C_{β} as a $p_{\pi}C$ center in WCBD pave the way for a new approach to the design of molecules and materials containing multiple $p_{\pi}C$ centers. Several such molecules have been proposed by extending the WCBD motif in 1-, 2- and 3-dimensions. The presence of 1,3-WC bond as well as metalloaromaticity in all these systems is established on the basis of the characteristic bond order, catastrophe ring critical point in QTAIM, ^{13}C -NMR values and various NICS indices. The 3-dimensional structures propose the formation of $p_{\pi}C$ incorporated metal-organic frameworks.

Acknowledgements

This work is supported by CSIR through the project CSC019 and PRR is thankful to UGC for the research fellowship.

References

- R. Hoffmann, R. W. Alder and C. F. Wilcox, *J. Am. Chem. Soc.*, 1970, **92**, 4992-4993.
- R. Hoffmann, *Pure Appl. Chem.*, 1971, **28**, 181-194.
- V. I. Minkin, R. M. Minyaev and R. Hoffmann, *Russ. Chem. Rev.*, 2002, **71**, 869-892.
- J. B. Collins, J. D. Dill, E. D. Jemmis, Y. Apeloig, P. v. R. Schleyer, R. Seeger and J. A. Pople, *J. Am. Chem. Soc.*, 1976, **98**, 5419-5427.
- P. v. R. Schleyer and A. I. Boldyrev, *J. Chem. Soc., Chem. Commun.*, 1991, 1536-1538.
- Z.-X. Wang and P. v. R. Schleyer, *J. Am. Chem. Soc.*, 2001, **123**, 994-995.
- F. A. Cotton and M. Millar, *J. Am. Chem. Soc.*, 1977, **99**, 7886-7891.
- R. H. Cayton, S. T. Chacon, M. H. Chisholm, M. J. Hampden-Smith, J. C. Huffman, K. Folting, P. D. Ellis and B. A. Huggins, *Angew. Chem. Int. Ed.*, 1989, **28**, 1523-1525.
- F. A. Cotton and E. S. Shamshoum, *J. Am. Chem. Soc.*, 1985, **107**, 4662-4667.
- P. Leoni, M. Pasquali, G. Pieri, A. Albinati, P. S. Pregosin and H. Rueegger, *Organometallics*, 1995, **14**, 3143-3145.
- W. J. Evans, R. A. Keyer and J. W. Ziller, *Organometallics*, 1993, **12**, 2618-2633.
- D. Röttger and G. Erker, *Angew. Chem. Int. Ed.*, 1997, **36**, 812-827.
- G. Erker, *Comments Inorg. Chem.*, 1992, **13**, 111-131.
- P. Arndt, C. Lefeber, R. Kempe, A. Tillack and U. Rosenthal, *Chemische Berichte*, 1996, **129**, 1281-1285.
- G. Erker, W. Fromberg, K. Angermund, R. Schlund and C. Kruger, *J. Chem. Soc., Chem. Commun.*, 1986, 372-374.
- R. Gleiter, I. Hyla-Kryspin, S. Niu and G. Erker, *Organometallics*, 1993, **12**, 3828-3836.
- M. R. Churchill, J. W. Ziller, J. H. Freudenberger and R. R. Schrock, *Organometallics*, 1984, **3**, 1554-1562.
- J. H. Freudenberger, R. R. Schrock, M. R. Churchill, A. L. Rheingold and J. W. Ziller, *Organometallics*, 1984, **3**, 1563-1573.
- M. R. Churchill and J. W. Ziller, *J. Organomet. Chem.*, 1985, **286**, 27-36.
- S. Roy, U. Rosenthal and E. D. Jemmis, *Acc. Chem. Res.*, 2014, **47**, 2917-2930.
- G. Erker, *Chem. Soc. Rev.*, 1999, **28**, 307-314.
- W. Siebert and A. Gunale, *Chem. Soc. Rev.*, 1999, **28**, 367-371.
- R. Keese, *Chem. Rev.*, 2006, **106**, 4787-4808.
- G. Merino, M. A. Méndez-Rojas, A. Vela and T. Heine, *J. Comput. Chem.*, 2007, **28**, 362-372.
- L.-M. Yang, E. Ganz, Z. Chen, Z.-X. Wang and P. v. R. Schleyer, *Angew. Chem. Int. Ed.*, 2015, **54**, 9468-9501.
- C. H. Suresh and G. Frenking, *Organometallics*, 2010, **29**, 4766-4769.
- C. H. Suresh and G. Frenking, *Organometallics*, 2012, **31**, 7171-7180.
- J. H. Wengrovius, J. Sancho and R. R. Schrock, *J. Am. Chem. Soc.*, 1981, **103**, 3932-3934.
- S. F. Pedersen, R. R. Schrock, M. R. Churchill and H. J. Wasserman, *J. Am. Chem. Soc.*, 1982, **104**, 6808-6809.
- S. Beer, C. G. Hrib, P. G. Jones, K. Brandhorst, J. Grunenberg and M. Tamm, *Angew. Chem. Int. Ed.*, 2007, **46**, 8890-8894.
- J. Zhu, G. Jia and Z. Lin, *Organometallics*, 2006, **25**, 1812-1819.
- S. Beer, K. Brandhorst, C. G. Hrib, X. Wu, B. Haberlag, J. Grunenberg, P. G. Jones and M. Tamm, *Organometallics*, 2009, **28**, 1534-1545.
- L. G. McCullough, M. L. Listemann, R. R. Schrock, M. R. Churchill and J. W. Ziller, *J. Am. Chem. Soc.*, 1983, **105**, 6729-6730.
- L. G. McCullough, R. R. Schrock, J. C. Dewan and J. C. Murdzek, *J. Am. Chem. Soc.*, 1985, **107**, 5987-5998.
- S. Roy, E. D. Jemmis, A. Schulz, T. Beveries and U. Rosenthal, *Angew. Chem. Int. Ed.*, 2012, **51**, 5347-5350.
- T. Woo, E. Folga and T. Ziegler, *Organometallics*, 1993, **12**, 1289-1298.
- Z. Lin and M. B. Hall, *Organometallics*, 1994, **13**, 2878-2884.
- C. H. Suresh and G. Frenking, *Organometallics*, 2013, **32**, 1531-1536.
- G. D. Geske and A. I. Boldyrev, *Inorg. Chem.*, 2002, **41**, 2795-2798.
- X. Li, H.-F. Zhang, L.-S. Wang, G. D. Geske and A. I. Boldyrev, *Angew. Chem. Int. Ed.*, 2000, **39**, 3630-3632.
- L.-m. Yang, Y.-h. Ding and C.-c. Sun, *J. Am. Chem. Soc.*, 2007, **129**, 658-665.

42. P. D. Pancharatna, M. A. Méndez-Rojas, G. Merino, A. Vela and R. Hoffmann, *J. Am. Chem. Soc.*, 2004, **126**, 15309-15315.
43. G.-L. Chai, C.-S. Lin and W.-D. Cheng, *J. Mater. Chem.*, 2012, **22**, 11303-11309.
44. M. Wu, Y. Pei and X. C. Zeng, *J. Am. Chem. Soc.*, 2010, **132**, 5554-5555.
45. A. Schäfer, C. Huber and R. Ahlrichs, *J. Chem. Phys.*, 1994, **100**, 5829-5835.
46. D. Andrae, U. Häußermann, M. Dolg, H. Stoll and H. Preuß, *Theoretica chimica acta*, 1990, **77**, 123-141.
47. J. P. Perdew, *Phys. Rev. B*, 1986, **33**, 8822-8824.
48. A. D. Becke, *Phys. Rev. A*, 1988, **38**, 3098-3100.
49. M. J. Frisch, G. W. Trucks, H. B. Schlegel, G. E. Scuseria, M. A. Robb, J. R. Cheeseman, G. Scalmani, V. Barone, B. Mennucci, G. A. Petersson, H. Nakatsuji, M. Caricato, X. Li, H. P. Hratchian, A. F. Izmaylov, J. Bloino, G. Zheng, J. L. Sonnenberg, M. Hada, M. Ehara, K. Toyota, R. Fukuda, J. Hasegawa, M. Ishida, T. Nakajima, Y. Honda, O. Kitao, H. Nakai, T. Vreven, J. A. Montgomery, Jr., J. E. Peralta, F. Ogliaro, M. Bearpark, J. J. Heyd, E. Brothers, K. N. Kudin, V. N. Staroverov, T. Keith, R. Kobayashi, J. Normand, K. Raghavachari, A. Rendell, J. C. Burant, S. S. Iyengar, J. Tomasi, M. Cossi, N. Rega, J. M. Millam, M. Klene, J. E. Knox, J. B. Cross, V. Bakken, C. Adamo, J. Jaramillo, R. Gomperts, R. E. Stratmann, O. Yazyev, A. J. Austin, R. Cammi, C. Pomelli, J. W. Ochterski, R. L. Martin, K. Morokuma, V. G. Zakrzewski, G. A. Voth, P. Salvador, J. J. Dannenberg, S. Dapprich, A. D. Daniels, O. Farkas, J. B. Foresman, J. V. Ortiz, J. Cioslowski, and D. J. Fox, *Gaussian 09, Revision D.01*, Gaussian, Inc., Wallingford CT, 2013.
50. T. K. Brunck and F. Weinhold, *J. Am. Chem. Soc.*, 1979, **101**, 1700-1709.
51. R. F. W. Bader, *Acc. Chem. Res.*, 1985, **18**, 9-15.
52. R. F. W. Bader, ed., *Atoms in molecules: A quantum theory*, Clarendon Press, Oxford, UK, , 1990.
53. T. A. Keith, TK Gristmill Software, Overland Park KS, USA, 2014 14.04.17 edn., 2014.
54. T. Helgaker, M. Jaszuński and K. Ruud, *Chem. Rev.*, 1999, **99**, 293-352.
55. K. Ruud, T. Helgaker, K. L. Bak, P. Jørgensen and H. J. R. A. Jensen, *J. Chem. Phys.*, 1993, **99**, 3847-3859.
56. P. v. R. Schleyer, C. Maerker, A. Dransfeld, H. Jiao and N. J. R. v. E. Hommes, *J. Am. Chem. Soc.*, 1996, **118**, 6317-6318.
57. D. Geuenich, K. Hess, F. Köhler and R. Herges, *Chem. Rev.*, 2005, **105**, 3758-3772.
58. R. Herges and D. Geuenich, *J. Phys. Chem. A*, 2001, **105**, 3214-3220.
59. M. E. O'Reilly, I. Ghiviriga, K. A. Abboud and A. S. Veige, *Dalton Trans.*, 2013, **42**, 3326-3336.
60. R. F. W. Bader, *J. Phys. Chem. A*, 1998, **102**, 7314-7323.
61. E. Cerpa, A. Krapp, A. Vela and G. Merino, *Chem. Eur. J.*, 2008, **14**, 10232-10234.
62. S. Grimme, C. Muck-Lichtenfeld, G. Erker, G. Kehr, H. D. Wang, H. Beckers and H. Willner, *Angew. Chem. Int. Ed.*, 2009, **48**, 2592-2595.
63. P. Dem'yanov and P. Polestshuk, *Chem. Eur. J.*, 2012, **18**, 4982-4993.
64. A. Guevara-Garcia, P. W. Ayers, S. Jenkins, S. R. Kirk, E. Echegaray and A. Toro-Labbe, in *Electronic Effects in Organic Chemistry*, ed. B. Kirchner, 2014, vol. 351, pp. 103-124.
65. A. Morgenstern, T. Wilson, J. Miorelli, T. Jones and M. E. Eberhart, *Comp. Theor. Chem.*, 2015, **1053**, 31-37.
66. J. Overgaard, H. F. Clausen, J. A. Platts and B. B. Iversen, *J. Am. Chem. Soc.*, 2008, **130**, 3834-3843.
67. L. J. Farrugia, C. Evans, D. Lentz and M. Roemer, *J. Am. Chem. Soc.*, 2009, **131**, 1251-1268.
68. P. R. Remya and C. H. Suresh, *Dalton Trans.*, 2015, **44**, 17660.
69. J. H. Freudenberger and R. R. Schrock, *Organometallics*, 1986, **5**, 1411-1417.
70. J. Feldman, W. M. Davis and R. R. Schrock, *Organometallics*, 1989, **8**, 2266-2268.
71. P. E. Romero and W. E. Piers, *J. Am. Chem. Soc.*, 2005, **127**, 5032-5033.
72. A. Lugo, J. Fischer and D. B. Lawson, *J. Mol. Struct.-THEOCHEM*, 2004, **674**, 139-146.
73. C. Zhu, S. Li, M. Luo, X. Zhou, Y. Niu, M. Lin, J. Zhu, Z. Cao, X. Lu, T. Wen, Z. Xie, P. v. R. Schleyer and H. Xia, *Nat Chem*, 2013, **5**, 698-703.
74. C. Q. Zhu, Y. H. Yang, M. Luo, C. X. Yang, J. J. Wu, L. N. Chen, G. Liu, T. B. Wen, J. Zhu and H. P. Xia, *Angew. Chem. Int. Ed.*, 2015, **54**, 6181-6185.
75. H. Masui, *Coord. Chem. Rev.*, 2001, **219-221**, 957-992.
76. F. Erdman and D. B. Lawson, *J. Organomet. Chem.*, 2005, **690**, 4939-4944.
77. U. Rosenthal, A. Ohff, A. Tillack, W. Baumann and H. Görls, *J. Organomet. Chem.*, 1994, **468**, C4-C8.
78. P.-M. Pellny, V. V. Burlakov, W. Baumann, A. Spannenberg, R. Kempe and U. Rosenthal, *Organometallics*, 1999, **18**, 2906-2909.
79. N. J. Long and C. K. Williams, *Angew. Chem. Int. Ed.*, 2003, **42**, 2586-2617.
80. T. Ren, *Organometallics*, 2005, **24**, 4854-4870.
81. W.-Y. Wong and C.-L. Ho, *Coord. Chem. Rev.*, 2006, **250**, 2627-2690.

Planar Tetracoordinate Carbon in Tungstenacyclobutadiene of Alkyne Metathesis and Expanded Structures

Premaja R. Remya and Cherumuttathu H. Suresh

Chemical Science and Technology Division, Academy of Scientific and Innovative Research (AcSIR), CSIR-National Institute for Interdisciplinary Science and Technology, Trivandrum, India, 695019

Graphical Abstract

Establishing the C_{β} of tungstenacyclobutadiene (WCBD) as a $_{pt}C$ center pave the way for a new strategy to make novel material containing multiple $_{pt}C$ centers. The 1-,2- and 3-dimensional expansion of the WCBD motifs provide access to $_{pt}C$ -incorporated new metal-organic frameworks.

